Protein Science (1993), *2*, 2177-2186. Cambridge University Press. Printed in the USA.

Divalent metal ions influence catalysis and active-site accessibility in the cAMP-dependent protein kinase

JOSEPH A. ADAMS AND SUSAN S. TAYLOR

Department of Chemistry, University of California at San Diego, La Jolla, California 92093-0654

(RECEIVED June 21, 1993; ACCEPTED September 1, 1993)

Abstract

Phosphorylation of the peptide LRRASLG by the catalytic subunit of cAMP-dependent protein kinase was measured in the presence of various divalent metals to establish the role of electrophiles in the kinetic mechanism. Under conditions of low or high metal concentrations, the apparent second-order rate constant, $k_{cat}/K_{peptide}$, and the maximal rate constant, k_{cat}, followed the trend $Mg^{2+} > Co^{2+} > Mn^{2+}$. Competitive inhibition studies indicate that the former effect is not due to destabilization of the substrate complex, E·ATP·S. The effects of solvent viscosity on the steady-state kinetic parameters were interpreted according to a simple mechanism involving substrate binding, phosphotransfer, and product release steps and two metal chelation sites in the nucleotide pocket. Decreases in k_{cat} and $k_{cat}/K_{peptide}$ result mostly from attenuations in the dissociation rate constant for ADP and the association rate constant for the substrate, respectively. Decreases in the phosphoryl transfer rate constant have only negligible to moderate effects on these parameters. The low observed values for the association rate constant of the substrate indicate that the metals control the concentration of the productive binary form, E_a·ATP, and indirectly the accessibility of the active site. By comparison, Mg^{2+} is the best divalent metal catalyst because it uniformly lowers the transition state energies for all steps in the kinetic mechanism, permitting maximum flux of substrate to product. The data suggest that cAMP-dependent protein kinase uses metal ions to serve multiple roles in facilitating phosphotransfer and accelerating substrate association and product dissociation.

Keywords: catalytic subunit; divalent metal ions; solvent viscosity; steady-state kinetics

Many theories have been proposed to explain the large rate enhancements by metal catalysts at the active sites of enzymes. Data attained from enzymatic and model studies suggest that metal ions may accelerate reactions by lowering the chemical transition state energy through polarization of the electrophile, charge reduction, and stabilization of the leaving group (Jencks, 1987). In addition, ions may confer tight binding or proper orientation of the substrate's functional groups. An efficient enzyme recognizes substrate, easily modifies it, and then quickly releases the product without populating unproductive or very stable intermediate species. Enzymes accomplish this by lowering the transition state energies of the chemical and conformational steps and equalizing the ground states of all bound species to maximize catalytic efficiency (Albery & Knowles, 1977). We have determined the effects of various divalent metal ions on a phosphotransferring enzyme, cAMP-dependent protein kinase, to understand better the role of metal ions in catalysis.

cAPK is a tetramer (R_2C_2) consisting of a regulatory dimer (R_2) and two catalytic subunits (C). The C-subunit is dissociated from the tetramer upon binding of cAMP to the regulatory dimer:

$$4\ \text{cAMP} + R_2C_2 \rightleftharpoons 4\ \text{cAMP-}R_2 + 2C. \qquad (1)$$

The active, free C-subunit then phosphorylates a number of cytoplasmic and nuclear-localized proteins on serine and threonine residues, eliciting a broad range of effects on cellular functions ranging from glucose metabolism to gene transcription (Krebs & Beavo, 1979). Studies with small peptides show that the C-subunit efficiently phosphorylates proteins that have the minimum consensus sequence R-R-X-S/T-hyd, where X is uncharged and hyd is a hydrophobic residue (Kemp et al., 1977; Zetterqvist

Reprint requests to: Susan S. Taylor, Department of Chemistry, University of California at San Diego, 9500 Gilman Drive, La Jolla, California 92093-0654.

Abbreviations: ADP, adenosine-5′-diphosphate; ATP, adenosine-5′-triphosphate; cAMP, adenosine cyclic 3′,5′-monophosphate; cAPK, cAMP-dependent protein kinase; NADH, nicotinamide adenine dinucleotide, reduced; Tris, tris(hydroxymethyl)aminomethane.

et al., 1990). Stereochemical studies suggest that the C-subunit transfers the γ phosphate of ATP via a direct, in-line displacement reaction (Ho et al., 1988), yet a hindered metaphosphate intermediate is still plausible. Although the transfer efficiency is best in the presence of Mg^{2+}, the enzyme will accept a number of other divalent metals (Bhatnagar et al., 1983). In the absence of metal ions, the enzyme has no detectable kinase activity (Armstrong et al., 1979).

Comprehensive steady-state kinetic analyses reveal that the C-subunit will phosphorylate the substrate, LRRASLG, by a random kinetic mechanism, although the initial binding of ATP is preferred (Cook et al., 1982; Kong & Cook, 1988). Comparison of K_d and K_m ($K_d > K_m$) for LRRASLG in the presence of an ATP analog and ATP, respectively, implies that a fast step, namely phosphotransfer, follows substrate binding. The results from studies on a wide range of peptide substrates reveal similar maximal velocities although K_m values vary greatly, indicating that the catalytic mechanism of the C-subunit exploits a common rate-determining step (Järv & Ragnarsson, 1991). The effects of solvent viscosity on the steady-state kinetic parameters verify that the rate of phosphoryl transfer greatly exceeds the rate of ADP release, the rate-determining step in k_{cat}, when the free concentration of Mg^{2+} is high (Adams & Taylor, 1992).

The effects of changes in solvent viscosity on the steady-state kinetic parameters for LRRASLG phosphorylation were measured under conditions of varying divalent metal concentrations. The three metals chosen—Mg^{2+}, Co^{2+}, and Mn^{2+}—bind tightly at the active site of the C-subunit and support catalysis, although at different levels (Bhatnagar et al., 1983). The present data were interpreted in light of a simple mechanism involving substrate binding, phosphotransfer, and product release steps. The active site of the C-subunit accommodates two metals: a primary, high-affinity metal site that chelates the β and γ phosphates and a secondary site that chelates the α and γ phosphates of ATP (Zheng et al., 1993a,b). The effects of the three metal replacements are discussed in terms of the individual rate constants for the kinetic mechanism, the metal occupancy of the nucleotide binding site, and the efficiency of catalysis. Decreases in k_{cat} or $k_{cat}/K_{peptide}$ due to the nature and concentration of the divalent metal ion are explained by attenuations in either the release rate of the product, ADP, or in the accessibility of the active site for substrate and the rates of phosphoryl transfer. This study illustrates that metal ions in cAPK are needed not only for the fast transfer of phosphate groups but also for rapid formation of the productive substrate complex and fast release of product.

Results

Steady-state kinetic parameters in the presence of divalent metals

The steady-state kinetic parameters, k_{cat}, $K_{peptide}$, and $k_{cat}/K_{peptide}$, for the phosphorylation of the peptide, LRRASLG, measured under conditions of saturating ATP and varied concentrations of $MgCl_2$, $MnCl_2$, or $CoCl_2$ are presented in Tables 1 and 2. High metal concentrations were achieved with 1 mM ATP and 11 mM $MnCl_2$, 2 mM ATP and 12 mM $CoCl_2$, or 2 mM ATP and 32 mM $MgCl_2$. Bhatnagar et al. (1983) showed by fluorescence polarization that the dissociation constants for Mg^{2+}, Mn^{2+}, and Co^{2+} and the secondary metal sites are 2.8, 0.03, and 0.06 mM, respectively. For these metals the affinity for the primary site is even higher when ATP is bound. Thus, all of the primary site and 90% or

Table 1. *Effects of divalent metals and solvent viscosity on k_{cat} for the phosphorylation of LRRASLG*[a]

Metal	Site	k_{cat} (s^{-1})	$(k_{cat})^{\eta}$	k_3 (s^{-1})[b]	k_4 (s^{-1})[b]
Mg^{2+}	1°	52 ± 1.7[c]	0.92 ± 0.21	≥235	56 ± 9
	1°/2°	14 ± 0.59[d]	1.0 ± 0.060	≥240	14 ± 1
Mn^{2+}	1°	13 ± 0.62[e]	0.40 ± 0.10	21 ± 2.8	32 ± 6.1
	1°/2°	0.93 ± 0.030[f]	0.85 ± 0.095	6.2 ± 3.9	1.1 ± 0.13
Co^{2+}	1°	17 ± 0.67[g]	0.44 ± 0.072	30 ± 4.0	38 ± 6.4
	1°/2°	5.4 ± 0.22[h]	0.82 ± 0.13	30 ± 20	6.6 ± 1.1

[a] Conditions: 1–5 mM ATP, 1.5–32 mM total metal, varying amounts of LRRASLG in 100 mM Tris, pH 8.0, in either the presence or absence of added viscosogen (see Materials and methods section), 24 °C.

[b] $k_3 = k_{cat}/[1 - (k_{cat})^{\eta}]$; $k_4 = k_{cat}/(k_{cat})^{\eta}$. These relationships are derived from Equation 2 and the maximum rate constant expression for the mechanism shown in Figure 3, $k_{cat} = k_3k_4/(k_3 + k_4)$.

[c] [ATP] = 5.0 mM; $[Mg^{2+}]^{tot}$ = 5.0 mM.

[d] [ATP] = 2.0 mM; $[Mg^{2+}]^{tot}$ = 32 mM.

[e] [ATP] = 3.0 mM; $[Mn^{2+}]^{tot}$ = 1.5 mM.

[f] [ATP] = 1.0 mM; $[Mn^{2+}]^{tot}$ = 11 mM.

[g] [ATP] = 5.0 mM; $[Co^{2+}]^{tot}$ = 4.0 mM.

[h] [ATP] = 2.0 mM; $[Co^{2+}]^{tot}$ = 5.0 mM.

Table 2. *Effects of divalent metals and solvent viscosity on $k_{cat}/K_{peptide}$ for the phosphorylation of LRRASLG*[a]

Metal	Site[b]	$k_{cat}/K_{peptide}$ ($mM^{-1}\ s^{-1}$)	$K_{peptide}$ (μM)	$(k_{cat}/K_{peptide})^{\eta}$	k_2[c] ($\mu M^{-1}\ s^{-1}$)
Mg^{2+}	1°	990 ± 140	52 ± 7.4	0.11 ± 0.09	9.0 ± 7.0
	1°/2°	320 ± 30	65 ± 11	0.13 ± 0.07	3.0 ± 2.0
Mn^{2+}	1°	107 ± 19	118 ± 20	0.14 ± 0.06	0.76 ± 0.35
	1°/2°	24 ± 2.9	39 ± 4.6	0.20 ± 0.088	0.12 ± 0.055
Co^{2+}	1°	477 ± 82	35 ± 5.8	0.33 ± 0.071	1.4 ± 0.38
	1°/2°	70 ± 11	77 ± 12	0.39 ± 0.13	0.18 ± 0.66

[a] Conditions: 1–5 mM ATP, 1.5–32 mM total metal, varying amounts of LRRASLG in 100 mM Tris, pH 8.0, in either the presence or absence of added viscosogen (see Materials and methods section), 24 °C.

[b] The specific concentrations of ATP and divalent metal ion needed to achieve these conditions are summarized in Table 1 (footnotes c–h).

[c] $k_2 = (k_{cat}/K_{peptide})/(k_{cat}/K_{peptide})^{\eta}$. This equation is derived from Equation 3 and the apparent second-order rate expression for the mechanism shown in Figure 3, $k_{cat}/K_{peptide} = k_2k_3/(k_{-2} + k_3)$.

more of the secondary site are bound at 30 mM free Mg^{2+} and at 10 mM free Mn^{2+} and Co^{2+}. The affinity of ATP (K_{ATP}) was measured under these metal concentrations and fixed peptide concentrations. At 64 and 96 μM peptide, $K_{ATP} = 11 \pm 4$ and 13 ± 2 μM when 10 mM free Mn^{2+} was used. At 162 μM peptide, $K_{ATP} = 102 \pm 21$ μM when 10 mM free Co^{2+} was used. Previous measurements of K_{ATP} in the presence of 10 mM free Mg^{2+} in 100 mM Tris, pH 8.0, were 18 ± 3.1 μM using 50 μM peptide (Adams & Taylor, 1992). Thus, 1–2 mM ATP is sufficient to saturate the enzyme under these metal concentrations.

The steady-state kinetic parameters were also measured under conditions that maximized occupancy of only the primary site. The observed initial velocity of the enzyme reaction as a function of total Mg^{2+} or Mn^{2+} and constant ATP concentrations was shown previously to be bimodal (Granot et al., 1980), indicating that two metal sites control activity. Occupancy of the primary site is absolutely required for activity, whereas occupancy of the secondary site is inhibitory. Because the affinity of Mg^{2+} for the two sites is sufficiently different (Bhatnagar et al., 1983), occupation of only the primary site is possible. However, only approximations could be made for optimal occupancy of this site for Mn^{2+} and Co^{2+}. To ensure that mostly the primary site is bound, k_{obs} was measured as a function of total metal concentration under both varied and fixed amounts of ATP and 400 μM LRRASLG (data not shown). The concentration of divalent metal and ATP at which a maximum velocity is achieved is assumed to represent the optimal conditions for single metal binding at the primary site. Tables 1 and 2 summarize the concentrations of ATP and metal and the respective k_{cat}, $K_{peptide}$, and $k_{cat}/K_{peptide}$ values associated with these conditions.

The coupled enzyme assay designed by Cook et al. (1982) worked well for all Mg^{2+} studies. However, significant lag phases were observed in the progress curves in the presence of either Mn^{2+} or Co^{2+}. This was not due to hysteresis, since increasing the pyruvate kinase concentration in the assay removed these effects. Presumably, the pyruvate kinase activity is lower in the presence of these metals, so the steady-state level of ADP is too high under turnover conditions. When higher pyruvate kinase concentrations are used, the observed initial velocity is proportional to the C-subunit concentration, indicating that the rate of the coupling enzymes is sufficiently fast relative to the enzyme reaction rate (data not shown).

Effects of solvent viscosity on the steady-state kinetic parameters

The steady-state kinetic parameters, k_{cat} and $k_{cat}/K_{peptide}$, for the phosphorylation of LRRASLG were measured in the presence of varying amounts of glycerol and sucrose. The ratio of these parameters in the absence and presence of added viscosogens was recorded as a function of relative viscosity (η^{rel}), using saturating ATP (1–5 mM) and varied free divalent metal concentrations in 100 mM Tris, pH 8.0. Figure 1 presents the viscosity-dependent steady-state kinetic data (k_{cat}) as a function of relative viscosity for low and high concentrations of free Mn^{2+}. Similar plots were made for k_{cat} and $k_{cat}/K_{peptide}$ in the presence of low and high Mg^{2+} and Co^{2+} concentrations (data not shown). The concentrations of divalent metal and ATP are listed in the footnotes of Tables 1 and 2. All data showed a linear relationship between the kinetic parameter and the relative solvent viscosity (data not shown). Tables 1 and 2 present the slopes of these plots ($(k_{cat})^{\eta}$ and $(k_{cat}/K_{peptide})^{\eta}$). All slope values fall between the theoretical limits of 0 and 1. The observed reaction velocities varied linearly with the C-subunit concentration, indicating that the added viscosogen and divalent metal did

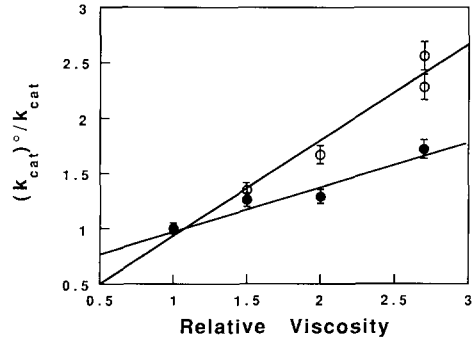

Fig. 1. Plot of $k_{cat}{}^o/k_{cat}$ for the phosphorylation of LRRASLG under conditions of low (●) and high (○) Mn^{2+} as a function of relative viscosity. $k_{cat}{}^o/k_{cat}$ is the ratio of the steady-state kinetic parameter under saturating ATP and varied substrate concentrations in the absence and presence of added viscosogen in 100 mM Tris, pH 8.0, 24 °C (see Materials and methods section). Low metal concentrations were achieved with 3.0 mM ATP and 1.5 mM $MnCl_2$. High metal concentrations were achieved with 1.0 mM ATP and 11 mM $MnCl_2$.

not affect the coupling enzymes' ability to measure the time-dependent production of ADP (data not shown).

Inhibitor binding studies

The peptide LRRNAI was shown previously to inhibit competitively the C-subunit's activity (Salerno et al., 1990). The dissociation constant of this inhibitor (K_I) was measured under several concentrations of divalent metal ions. Varying amounts of LRRNAI and metal, saturating ATP (1–5 mM), and fixed C-subunit were pre-equilibrated before initiating the reaction with LRRASLG. Table 3 summarizes the K_I values for this inhibitor under several concentrations of divalent metal ion.

Discussion

The C-subunit of cAPK has two coordination centers for divalent metal ions near the triphosphate moiety of ATP in the nucleotide binding site. The recent crystallographic solution of the recombinant C-subunit with ATP and an inhibitor peptide bound at the active site shows discernible electron density for two Mg^{2+} ions near the nucleotide (Zheng et al., 1993a). The ternary enzyme complex crystallized with high Mn^{2+} concentrations also shows two metal binding sites (Zheng et al., 1993b). Figure 2 shows the orientation of the two Mn^{2+} ions with respect to the triphosphate tail of ATP. The primary metal chelates the β and γ phosphates of ATP and the invariant Asp 184 of the C-subunit. The secondary metal coordinates the α and γ phosphates and the side chain of Asn 171. Extensive kinetic studies indicate that the primary metal is required for activity, while occupation of the secondary site causes a fourfold reduction in k_{cat} when Mg^{2+} is the varied metal (Cook et al., 1982). A similar kinetic effect was observed for Mn^{2+} substitution (Armstrong et al., 1979). Consequently, the second metal site is called the "inhibitory" site. We have found similar kinetic behavior for the recombinant C-subunit upon divalent metal ion replacement. The steady-state kinetic parameters were measured at the maxima and minima in the plots of k_{obs} versus total metal concentration and are listed in Tables 1 and 2. These values are consistent with previously published data for Mg^{2+} and Mn^{2+} (Armstrong et al., 1979; Cook et al., 1982). This metal ion effect on k_{cat} is also accompanied by tighter binding of ATP and ADP. Cook et al. (1982)

Table 3. *Dissociation constants for the competitive inhibitor LRRNAI under varying metal concentrations*[a]

Metal	Site[b]	K_I (μM)
Mg^{2+}	1°	160 ± 23
	1°/2°	520 ± 30
Mn^{2+}	1°	140 ± 28
	1°/2°	290 ± 53
Co^{2+}	1°	140 ± 22
	1°/2°	190 ± 38

[a] Conditions: 1–5 mM ATP, 1.5–32 mM total metal, fixed amounts of LRRASLG, and varying amounts of LRRNAI in 100 mM Tris, pH 8.0, 24 °C.

[b] The specific concentrations of ATP and divalent metal ion needed to achieve these conditions are summarized in Table 1 (footnotes c–h).

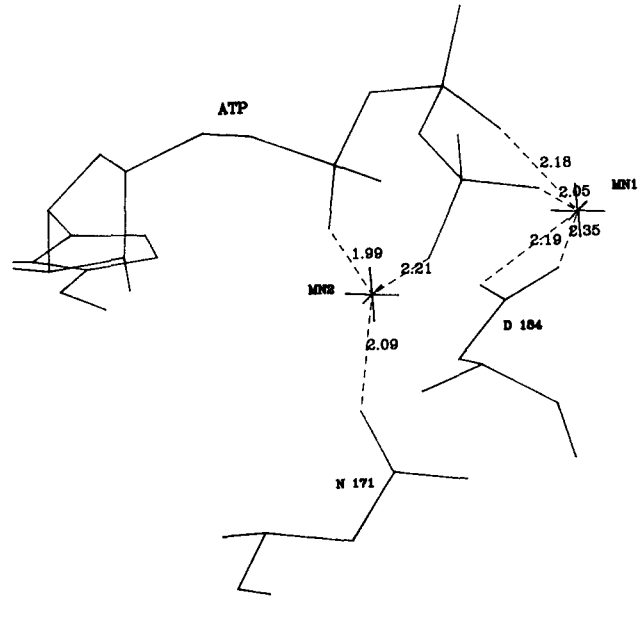

Fig. 2. Orientation of Mn^{2+} ions at the nucleotide binding site of the recombinant C-subunit co-crystallized with ATP and the inhibitor peptide PKI(5–24). MN1 and MN2 refer to the primary and secondary Mn^{2+} ions. The dashed lines and the associated numbers are the distances in Å. This structural representation was taken from Zheng et al. (1993b).

measured K_m values for ATP of 100 and 13 μM at 0.5 and 10 mM free Mg^{2+} in the absence of KCl.

Enzymes use a number of nonpeptidic molecules, including metal ions and vitamin-derived coenzymes, to lower the transition state energy for chemical transformations. Electrophilic catalysis is essential for many enzyme-promoted reactions, including carbon dioxide hydration, peptide bond hydrolysis, and carbonyl reductions. In addition to the specific role of metals in transition state stabilization, they are also important for substrate binding. The C-subunit uses divalent metals both to bind ATP and support phosphoryl transfer of the γ phosphate to hydroxylic acceptors. In the absence of the metal no catalysis is observed and the affinity of ATP is reduced by two to three orders of magnitude (Armstrong et al., 1979). Our study of the mechanism of catalysis for this enzyme by metal substitution and viscosity methods is aimed at answering two relevant questions: (1) Why is Mg^{2+} the preferred metal for supporting phosphotransfer in this protein kinase? and (2) What are the individual rate effects on the catalytic mechanism for substitution at the primary and the secondary metal positions? We have studied the consequences of three metal variants—Mg^{2+}, Mn^{2+}, Co^{2+}—at the nucleotide binding site and have measured their distinct effects on substrate and product binding and phosphoryl transfer steps.

Catalytic mechanism of the C-subunit

The catalytic mechanism of the C-subunit of cAPK was studied by a number of biochemical techniques. Peptide studies show that the C-subunit will phosphorylate serine and threonine residues when one or more basic residues are positioned N-terminal to the site of phosphotransfer (Kemp et al., 1977; Zetterqvist et al., 1990). Kinetic studies using the substrate LRRASLG showed that the mechanism is steady-state random, although the initial binding of ATP is preferred (Kong & Cook, 1988). The rate-determining step in the mechanism is the release of the product, ADP, when the Mg^{2+} concentrations are high (Adams & Taylor, 1992). The dissociation rate constant for the phosphorylated peptide and the rate of phosphoryl transfer are fast relative to k_{cat}. The chemical transfer is likely to involve direct, nucleophilic displacement of the γ phosphate of ATP by the serine hydroxyl group based on stereochemical precedence (Ho et al., 1988). Studies with altered peptide sequences showed no kinetic evidence of general-base catalysis (Adams & Taylor, 1993), although a conserved carboxyl side chain (Asp 166) is positioned near what would be the serine residue of the peptide in the X-ray crystal structure (Knighton et al., 1991a,b). Replacement of this residue in the yeast protein kinase yields a mutant enzyme form defective in k_{cat} (300-fold reduction) but unaffected in binding ATP and substrate (Gibbs & Zoller, 1991).

Effects of metal substitution on the kinetic mechanism

Viscosity studies were used previously to estimate the rate of phosphoryl transfer relative to k_{cat} when Mg^{2+} was bound at both the primary and secondary sites in the C-subunit (Adams & Taylor, 1992). If the relative viscosity of the solvent is increased by added glycerol or sucrose, both k_{cat} and $k_{cat}/K_{peptide}$ decrease in a manner consistent with the Stokes–Einstein relationship. A maximal effect of viscosity on k_{cat} is observed when ATP is saturating, implying that this parameter is limited by a diffusion-controlled step, namely product release (Adams & Taylor, 1992). The rate of phosphoryl transfer exceeds k_{cat} by at least 10-fold. This analysis was used for characterization of the C-subunit-catalyzed phosphorylation of the peptide LRRASLG when Mg^{2+}, Mn^{2+}, and Co^{2+} occupy the primary and both the primary and secondary sites in the nucleotide pocket.

When ATP concentrations are saturating the kinetic mechanism for the phosphorylation of the peptide can be written as shown in Figure 3. In this mechanism, the peptide combines with the E·ATP complex to form the active central complex, E·ATP·S, by the second-order association rate constant, k_2, and the dissociation rate constant, k_{-2}. The catalytic step, k_3, is the unimolecular rate constant that describes the chemical transfer of the γ phosphate of ATP to the hydroxyl functional group of the substrate as well as any viscosity-independent conformational changes associated with this transfer. The dissociation of the phosphorylated peptide (P) is also included in this step because its K_d is 100-fold larger than that for ADP (Cook et al., 1982; Whitehouse et al., 1983) and is not likely to limit the overall rate of product release. Consequently, k_4 refers to the dissociation rate constant of ADP alone. Because the diffusional rate constants k_2, k_{-2}, and k_4 are inversely proportional to the intrinsic solvent viscosity (Caldin, 1964), the ratio of these rate constants in the absence and presence of viscosogen is equal to the relative viscosity of the solvent (η^{rel}). By substituting this equality into the initial rate equation that defines the mechanism shown in Figure 3, a linear function of the ratio of the steady-state kinetic parameters in the absence and presence of viscosogen versus η^{rel} is obtained. Equations 2 and 3 define the slope of these relationships for k_{cat} and $k_{cat}/K_{peptide}$:

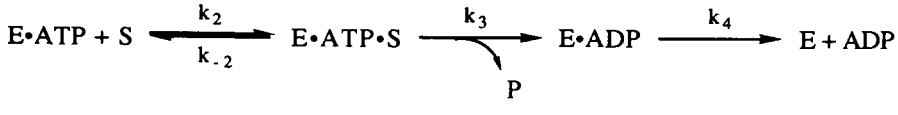

Fig. 3. Kinetic mechanism for phosphorylation of the peptide LRRASLG when ATP concentrations are saturating.

$$(k_{cat})^{\eta} = \frac{k_3}{k_3 + k_4} \quad (2)$$

$$(k_{cat}/K_{peptide})^{\eta} = \frac{k_3}{k_{-2} + k_3}, \quad (3)$$

where $(k_{cat})^{\eta}$ and $(k_{cat}/K_{peptide})^{\eta}$ are the slopes of the plots of $k_{cat}{}^{o}/k_{cat}$ and $(k_{cat}/K_{peptide})^{o}/k_{cat}/K_{peptide}$ versus η^{rel}, respectively. The superscript postscript "o" refers to the steady-state kinetic parameter in the absence of viscosogen. These slope values lie between the theoretical limits of 0 and 1 and give information on the contribution of product dissociation to the rate-determining step in k_{cat} and the stickiness of the substrate.

When $(k_{cat})^{\eta} \approx 1$, the chemical step ($k_3$) is fast and product dissociation (k_4) is the rate-determining step in k_{cat}. Low values for $(k_{cat})^{\eta}$ imply that the chemical step is slow relative to product release. When $(k_{cat}/K_{peptide})^{\eta} \approx 1$, the peptide is "sticky" and is phosphorylated faster than it can dissociate from the ternary complex (E·ATP·S). If Equations 2 and 3 are combined with the initial rate expressions for k_{cat} and $k_{cat}/K_{peptide}$, the rate constants in Figure 3 either can be calculated directly or an upper bound can be placed on them. Tables 1 and 2 list the values for these rate constants as a function of the ion bound. When Mg^{2+} is in the primary and secondary sites, the chemical step is fast relative to ADP dissociation. Owing to the measurement error of the viscosity effect on k_{cat} ($(k_{cat})^{\eta}$), only a lower limit can be placed on k_3 (Table 1). Moreover, the dissociation of the product, ADP, is rate-determining ($k_{cat} \approx k_4$) regardless of the Mg^{2+} occupancy. We presume that the dissociation rate constant for ADP is lower than that for the phosphorylated peptide despite the nature and concentration of the divalent metal. The correspondence between K_I and the dissociation rate constant for ADP supports this presumption. Cook et al. (1982) measured K_I's of 40 and 10 μM for ADP at low and high Mg^{2+} concentrations. This fourfold drop in K_I is mirrored by a fourfold decrease in the release rate of ADP (compare 56 and 14 s^{-1}; Table 2).

The effect of substituting Mn^{2+} or Co^{2+} at either the primary or secondary sites is to lower the rate of phosphoryl transfer by at least eightfold compared to that for Mg^{2+} (Table 1). No large effects are seen on the chemical transfer rate when the secondary site is occupied compared to the primary site for all three metals. Furthermore, metal substitution has little effect on the observed rate for ADP release when the metals bind only the primary site. This is an approximation for Mn^{2+}, because the primary and secondary sites have similar affinities for the ADP complex as measured by electron spin resonance (Armstrong et al., 1979). Thus, the dissociation rate constant for this ligand when Mn^{2+} concentrations are low is only a lower limit. It is not clear whether this is also true for Co^{2+} replacement. Nonetheless, Mn^{2+} binds 10 times more tightly to the primary site compared to the secondary site when ATP is bound, so the rates measured for phosphoryl transfer (k_3) are more reliable. Marked decreases in k_4 are observed when the secondary site is fully occupied for all metals. The largest effect is observed in the case of Mn^{2+}. Occupancy of the secondary site by this metal decreases the off rate of ADP greater than 30-fold. For Co^{2+} and Mn^{2+}, chemistry and product release equally contribute to the rate-determining step in k_{cat} when metal concentrations are low. ADP release predominantly controls k_{cat} when the primary and secondary sites are bound. Overall, the inhibitory effect of the secondary site on k_{cat} for all three metals is caused mostly by the slower dissociation rate of the product, not by large rate effects on the chemical step. Any changes in the rates of phosphoryl transfer with increasing metal concentrations are either insignificant relative to k_{cat} (as in the case of Mn^{2+}) or unmeasurable (as in the case of Mg^{2+}).

The concentration of productive E·ATP complex is low

Table 2 lists the observed association rate constants for the substrate extracted from the viscosity data. In general, the accessibility of the active site is higher when Mg^{2+} is used compared to Mn^{2+} and Co^{2+}. Nonetheless, the observed values of k_2 are well below the diffusion-controlled limit of $\approx 10^8$ M^{-1} s^{-1} for the binding of small ligands to enzymes (Hammes & Schimmel, 1970). The observed on rate for substrate measured by isotope partitioning methods (Kong & Cook, 1988) is also lower than expected. Because only the temperature and viscosity of the solvent are expected to alter diffusion if the electric potentials of the substrate and enzyme are unchanged upon metal substitution (Caldin, 1964), the observed values (Table 2) must represent a composite term of substrate dependent and independent steps. Although the CD spectra of various peptide/C-subunit complexes give evidence for conformational changes in secondary structure upon ligand binding (Reed et al., 1985), steps after the ternary complex (E·ATP·S) formation cannot account for a decreased association rate constant. Incorporation of a conformational change after ternary formation does not alter the solution of the viscosity dependent parameter, $k_{cat}/K_{peptide}$, so that a true rate constant is still obtained.[1]

[1] For a mechanism that involves an equilibrium change after ternary complex formation, the steady-state kinetic and viscosity dependent parameters are

$$k_{cat}/K_{peptide} = k_2 k_3 K_{eq}/(k_{-2} + k_3 K_{eq})$$

and

$$(k_{cat}/K_{peptide})^{\eta} = k_3 K_{eq}/(k_{-2} + k_3 K_{eq}),$$

where k_2 and k_{-2} are the association and dissociation rate constants for the substrate, K_{eq} is the equilibrium constant for the conformation change, and k_3 is the same as in Figure 3. Division of $k_{cat}/K_{peptide}$ by $(k_{cat}/K_{peptide})^{\eta}$ still gives the true rate constant, k_2.

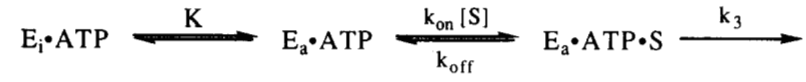

Fig. 4. Pathway for binding of the peptide substrate to only the productive complex, when two forms of the binary ATP complex have equilibrated in solution.

To explain the low values for k_2 in Figure 3, we propose that two forms of the binary ATP complex equilibrate in solution. The peptide substrate binds only the productive complex. This pathway is shown in Figure 4, where k_{on} and k_{off} are the association and dissociation rate constants for the substrate and the active binary enzyme ($E_a \cdot ATP$), K is the equilibrium constant for the formation of productive binary complex ($K = [E_a \cdot ATP]/[E_i \cdot ATP]$), and k_3 is the same as in Figure 3. In this mechanism, $K < 1$.[2] The second-order rate constant, $k_{cat}/K_{peptide}$, for the pathway shown in Figure 4 is

$$k_{cat}/K_{peptide} = \frac{k_{on}k_3K/(1 + K)}{k_{off} + k_3}. \quad (4)$$

If k_{on} and k_{off} are viscosity dependent, the slope of the ratio of $k_{cat}/K_{peptide}$ in the absence and presence of viscosogen versus η^{rel} is given by

$$(k_{cat}/K_{peptide})^{\eta} = \frac{k_3}{k_{off} + k_3}. \quad (5)$$

The ratio of Equations 4 and 5 indicates that the true association rate constant will be attenuated by the unfavorable equilibrium constant, K ($k_{on}^{obs} \approx k_{on} \cdot K$). Since the observed association rate constant for substrate at high Mg^{2+} is 3 μM^{-1} s^{-1} (Table 2) and the approximate rate for diffusion at 25 °C is 10^8 M^{-1} s^{-1}, we measured a value of K that is approximately 0.03.

The lower values of k_2 in Table 2 for metal replacement can be explained by further decreases in this equilibrium constant. Thus, the nature and concentration of the divalent metal must control the population of productive binary enzyme ($E_a \cdot ATP$), which is approximately 3% of the total enzyme concentration at high ATP levels. For the substitution of Mg^{2+} with Mn^{2+} and Co^{2+}, this percentage drops 25- and 17-fold, respectively, when the metal concentrations are high and 12- and 6-fold, respectively, when the concentrations are low. These values are derived from the relative decreases in k_2 (Table 2) upon Mg^{2+} replacement, assuming a constant value for the true association rate constant. The decrease in the active population of binary species is reflected in decreases in $k_{cat}/K_{peptide}$ (Table 2). For the substitution of Mg^{2+} with Mn^{2+} and Co^{2+}, the relative values of $k_{cat}/K_{peptide}$ decrease 13- and 5-fold, respectively, at high metal concentrations and 9- and 2-fold, respectively, at low concentrations. The lower relative values for changes in $k_{cat}/K_{peptide}$ compared to those for k_2 are due to the participation of both the substrate dissociation and phosphoryl rate constants in Equation 4. The observed decreases in k_2 are slightly offset in $k_{cat}/K_{peptide}$ by small increases in substrate stickiness (i.e., k_3/k_{off} in Fig. 4). Nonetheless, the majority of the observed reductions in $k_{cat}/K_{peptide}$ arise from decreases in k_2.

The phosphorylation reaction outlined in Figure 4 bears a resemblance to an "induced-fit" mechanism in that the enzyme is partitioned between an abundant, unproductive complex and a scarcely populated, productive species. However, the restrictive binding of the substrate to the latter species does not provide a pathway for substrate induction, a tenet of the "induced-fit" model (Koshland, 1958). Because substrate cannot bind $E_i \cdot ATP$, it cannot elicit the conformational changes needed for coordinating the active-site residues in the productive ternary complex. An outcome of this mechanism is that maximum catalytic efficiency as judged by $k_{cat}/K_{peptide}$ will be limited always by the equilibrium between the conformers regardless of the subsequent steps in the reaction (Equation 4). We are hesitant to speculate upon the molecular nature of the conformational change without detailed structural information on the binary $E \cdot ATP$ complex.

Two recent studies of the structure of the C-subunit suggest that domain movement may be relevant for substrate binding and catalysis. Firstly, Zheng et al. (1993b) solved the structure of a mammalian C-subunit co-crystallized with the inhibitor peptide PKI(5–24). This structure is larger than the recombinant binary and ternary complexes due to a rotation of the nucleotide domain relative to the peptide binding domain. This structural heterogeneity provides a more open conformation to allow the association of ATP even in the presence of inhibitors and substrates. Secondly, Olah et al. (1993) showed by small angle X-ray scattering and Fourier transform infrared spectroscopy that a 9% decrease in the radius of gyration of the C-subunit accompanies inhibitor binding. The lack of any changes in secondary structure led these authors to propose that domain movement is the likely cause. It is apparent from these structural studies and the kinetic findings of this paper that the C-subunit is flexible in both the apo- and ATP-bound enzyme forms. It is not yet obvious, though, what these structural changes are and how metal substitution controls this movement when ATP is bound.

Divalent metal substitution and catalytic efficiency

Although the catalytic subunit of cAPK will phosphorylate peptide substrates in the presence of a number of di-

[2] If K is large, the mechanism is kinetically indistinguishable from that shown in Figure 3, and a true rate constant would be measured.

valent metals, the kinase is most active in the presence of Mg^{2+} (Bhatnagar et al., 1983). When ATP concentrations are high, we have found that $k_{cat}/K_{peptide}$ decreases in the order $Mg^{2+} > Co^{2+} > Mn^{2+}$ (Table 2). The K_m for ATP was little affected by Mn^{2+} substitution and increased only fivefold by Co^{2+} substitution when the free concentration of metal ions was 10 mM. These effects, though, are negligible from a physiological standpoint because the concentration of ATP within the cell will normally exceed the measured K_m values and will not greatly fluctuate owing to the efficiency of adenylate kinase. No significant changes in $K_{peptide}$ were observed for each metal replacement regardless of the site. Comparison of the K_I values of the competitive inhibitor LRRNAI under low and high concentrations of metal (Table 3) indicates that Mn^{2+} and Co^{2+} substitution does not further destabilize the substrate ternary complex (E·ATP·S) provided that this inhibitor is a good analogue for the substrate. This is a good assumption because the K_I's for LRRNAI are close in value to the K_d's for LRRASLG and LRRAALG (Whitehouse et al., 1983). The inhibitor binds as well in the presence of Mn^{2+} or Co^{2+} as in the presence of Mg^{2+}. In fact, occupancy of the secondary site by Mn^{2+} or Co^{2+} has a small stabilizing effect on the inhibitor complex relative to Mg^{2+}. High concentrations of these former metals do not increase K_I as do increased amounts of Mg^{2+}. Thus, we can evaluate any changes in the specificity term, $k_{cat}/K_{peptide}$, of the enzyme by changes in the rate constants for phosphoryl transfer and substrate association upon metal ion substitution.[3]

A useful way of demonstrating the overall effects of metal ion substitution on the kinetic mechanism of the C-subunit is to construct a free energy profile for the enzyme reaction. Figure 5 illustrates the effects of varying metal on the transition state energies of the chemical, substrate binding, and product release steps when either metal sites are occupied and ATP concentrations are high. For this comparison, the internal equilibrium for phosphotransfer was assumed constant and was set at 100 based on pH-corrected values of the overall reaction equilibrium constant and the dissociation constants of all substrates and products (Qamar et al., 1992). The K_I values for the competitive inhibitor LRRNAI were used to set the ground state energies of the E·ATP and E·ATP·S complexes (Fig. 3). As stated in the previous section, this latter equilibrium comprises both the unfavorable equilibrium between unproductive and productive binary forms and substrate binding ($E_i \cdot ATP \rightarrow E_a \cdot ATP \cdot S$). A concentration of 50 μM was used as a standard state for the substrate LRRASLG. The net effect of replacing Mg^{2+} with other divalent metal ions at high concentrations is uniform destabilization of the transition state energies for all three steps in Figure 3 relative to the ground state energies (Fig. 5B). At low concentration of metal, the observed association and phosphoryl transfer rate constants are affected (Fig. 5A). The observed dissociation rate constant for ADP does not appear to be altered by replacement. However, any specific effect on this rate constant may be masked by the inability to bind cleanly the primary site only in the case of Mn^{2+} and Co^{2+} so that the three metals may stabilize the product release steps. From the free energy profiles of Figure 5 we can see

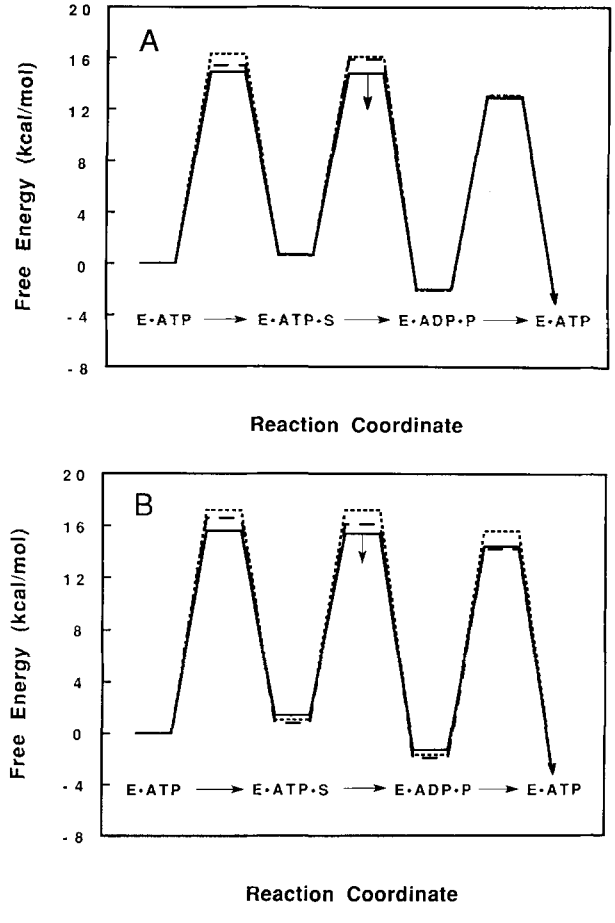

Fig. 5. Free energy reaction profile for the phosphorylation of LRRASLG at high ATP concentrations in 100 mM Tris, pH 8.0, 24 °C, when divalent metal concentrations are low (**A**) or high (**B**) for Mg^{2+} (——), Mn^{2+} (· · · ·), and Co^{2+} (----). The footnotes of Table 1 list the concentrations of metal and ATP needed to achieve binding with the primary or binding with the primary and secondary sites. The concentration of LRRASLG was set at 50 μM, and the ground state energy of the E·ATP·S complex was set according to the K_I values of Table 3. The free energy of the E·ATP complex was arbitrarily set at zero. The internal equilibrium constant was set at 100 based on ^{31}P NMR data (Qamar et al., 1992). The free energies of the individual transition state energies were calculated from the Erying equation and the rate constant data of Tables 1 and 2. The arrows below the transition states for phosphotransfer in the presence of Mg^{2+} indicate that these are upper boundaries.

[3] For the scheme shown in Figure 3, $k_{cat}/K_{peptide} = k_3/(K_d + k_3/k_2)$. If we assume that the K_d for the substrate is equivalent to the K_I for the inhibitor, then only k_3 and/or k_2 will affect $k_{cat}/K_{peptide}$ when ATP concentrations are high.

clearly that the general effects of each metal on the steady-state kinetic parameters are distributed throughout the kinetic mechanism and are not localized to any one bi- or unimolecular step. These results emphasize the dual importance of metal ions in modulating both catalytic and binding events in cAPK. The free energy profile of Figure 5A most closely represents the energy changes expected under physiological conditions. Not surprisingly, all transition state energies under low metal ion concentration are smaller than those at high concentrations.

Conclusions

The data presented here define the role of electrophiles in the phosphorylation of peptides by cAPK. The effects of metal concentration and type on the steady-state kinetic parameters are rationalized by a simple phosphorylation scheme involving substrate binding, chemical transfer, and ADP dissociation. Good metal ions such as Mg^{2+} impart their catalytic power by uniformly lowering the transition state energies of all steps in the reaction, not only the phosphotransfer step. In fact, decreases in the rate of chemistry do not greatly influence the steady-state kinetic parameters. Attenuations in k_{cat} and $k_{cat}/K_{peptide}$ are largely the results of decreases in the rate constants for ADP release and substrate association, respectively. The latter effect is due to the partitioning of the ATP-bound complex between a productive and an unproductive form. The net result is an apparent reduction in the accessibility of the active site for peptide substrates. This study suggests that increases in catalytic efficiency are possible through productive enzyme formation but only at the cost of decreased enzymic flexibility. This may be a burdensome attribute for protein kinases such as cAPK that must accept a diverse battery of protein substrates in its active site.

Materials and methods

Materials

ATP, phosphoenolpyruvate, magnesium chloride, NADH, Tris, pyruvate kinase (rabbit muscle), and lactate dehydrogenase (bovine heart) were purchased from Sigma. Sucrose and manganese chloride were purchased from Mallinckrodt. Cobalt chloride and glycerol were purchased from Fisher Scientific.

Peptides and protein

The peptides LRRASLG and LRRNAI were synthesized at the Peptide and Oligonucleotide Facility at the University of California, San Diego, and were purified by reverse-phase preparative HPLC. The concentration of LRRASLG peptides was determined by complete turnover with the catalytic subunit under conditions of limiting peptide. The concentration of LRRNAI was determined from its molecular weight. The recombinant C-subunit was expressed and purified from *Escherichia coli* according to previously published procedures (Yonemoto et al., 1991). The concentration of enzyme was measured by A_{280} ($A_{0.1\%} = 1.2$).

Kinase assay

The activity of the C-subunit was measured spectrophotometrically by coupling ADP production with NADH oxidation by pyruvate kinase and lactate dehydrogenase (Cook et al., 1982). Typically, 1–5 mM ATP and 1.5–32 mM $MgCl_2$, $CoCl_2$, or $MnCl_2$ were pre-equilibrated with the catalytic subunit in a buffer containing 1 mM phosphoenolpyruvate, 0.3 mM NADH, lactate dehydrogenase (4 units), and pyruvate kinase (4–24 units). The higher amounts of pyruvate kinase (>4 units) were used for kinase reactions with Mn^{2+} or Co^{2+}. Reactions were initiated by adding varying amounts of peptide. The dissociation constants of LRRNAI in the presence of varying metals were measured by pre-equilibrating the enzyme, saturating ATP and varied inhibitor concentrations, and initiating the reaction with fixed amounts of LRRASLG. All reactions were done in 100 mM Tris, pH 8.0, in either the presence or absence of glycerol or sucrose at 24 °C.

Solution viscosity measurements

The relative viscosity (η^{rel}) of buffers containing glycerol or sucrose was measured relative to a 100 mM Tris buffer at pH 8.0, 24.0 °C, using an Ostwald viscometer (Shoemaker & Garland, 1962). Glycerol buffers (25% and 40%, w/w) were used to obtain relative viscosity values of 1.5 and 2.0, respectively. A 40% (w/w) sucrose solution was used to obtain a relative viscosity of 2.7. All measurements of viscosity were performed in triplicate.

Data analysis

The values of V_{max} and $K_{peptide}$ were determined from plots of initial velocity versus substrate concentration according to Equation 6:

$$v^0 = \frac{V_{max}[S]}{[S] + K_{peptide}}, \tag{6}$$

where v^0 is the initial velocity, [S] is the concentration of the varied substrate, V_{max} is the maximal velocity, and $K_{peptide}$ is the Michaelis constant. The maximal velocity was then converted to k_{cat} by dividing V_{max} by the total enzyme concentration. The apparent K_I values ($^{app}K_I$) for the competitive inhibitor LRRNAI were measured by plotting the reciprocal of the initial reaction velocity ($1/v^0$) versus the inhibitor concentration in a Dixon

plot (Segel, 1975). The true K_I values were then calculated from the fixed substrate concentration and $K_{peptide}$ ($^{app}K_I = K_I(1 + [S]/K_{peptide})$).

Acknowledgments

We thank Dr. Patricia Jennings for critical reading of this manuscript. We also thank Siv Garrod for the HPLC purification of the peptides and Karen Prather for the purification of the catalytic subunit. This work was supported by NIH research grant GM 19301-20 to S.T. and NIH research grant GM 14528-02 to J.A.

References

Adams, J.A. & Taylor, S.S. (1992). Energetic limits of phosphotransfer in the catalytic subunit of cAMP-dependent protein kinase as measured by viscosity experiments. *Biochemistry 31*, 8516-8522.

Adams, J.A. & Taylor, S.S. (1993). Phosphorylation of peptide substrates for the catalytic subunit of cAMP-dependent protein kinase. *J. Biol. Chem. 268*, 7747-7752.

Albery, W.J. & Knowles, J.R. (1977). Efficiency and evolution of enzyme catalysis. *Angew. Chem. Int. Ed. Engl. 16*, 285-293.

Armstrong, R.N., Kondo, H., & Kaiser, E.T. (1979). Magnetic resonance and kinetic studies of the manganous (II) ion and substrate complexes of the catalytic subunit of adenosine 3',5'-monophosphate dependent protein kinase from bovine heart. *Proc. Natl. Acad. Sci. USA 76*, 722-725.

Bhatnagar, D., Roskoski, R., Jr., Rosendahl, M.S., & Leonard, N.J. (1983). Adenosine cyclic 3',5'-monophosphate dependent kinase: A new fluorescence displacement titration technique for characterizing the nucleotide binding site on catalytic subunit. *Biochemistry 22*, 6310-6317.

Caldin, E.F. (1964). *Fast Reactions in Solution*, pp. 10-11. Wiley, New York.

Cook, P.F., Neville, M.E., Jr., Vrana, K.E., Hartl, F.T., & Roskoski, R., Jr. (1982). Adenosine cyclic 3',5'-monophosphate dependent protein kinase: Kinetic mechanism for the bovine skeletal muscle catalytic subunit. *Biochemistry 21*, 5794-5799.

Gibbs, C.S. & Zoller, M.J. (1991). Rational scanning mutagenesis of a protein kinase identifies functional regions involved in catalysis and substrate interactions. *J. Biol. Chem. 266*, 8923-8931.

Granot, J., Mildvan, A.S., Bramson, H.N., & Kaiser, E.T. (1980). Magnetic resonance measurements of intersubstrate distances at the active site of protein kinase using substitution-inert cobalt (III) and chromium (III) complexes of adenosine 5'-(β, γ-methylenetriphosphate). *Biochemistry 19*, 3537-3543.

Hammes, G.G. & Schimmel, P.R. (1970). Rapid reactions and transient states. In *Enzymes*, 3rd Ed., Vol. 2 (Boyer, P.D., Ed.), pp. 67-114. Academic Press, New York.

Ho, M.-F., Bramson, H.N., Hansen, D.E., Knowles, J.R., & Kaiser, E.T. (1988). Stereochemical course of the phospho group transfer catalyzed by cAMP-dependent protein kinase. *J. Am. Chem. Soc. 110*, 2680-2681.

Järv, J. & Ragnarsson, U. (1991). Linear free energy relationships in cAMP-dependent protein kinase reactions with synthetic substrates. *Bioorgan. Chem. 19*, 77-87.

Jencks, W.P. (1987). *Catalysis in Chemistry and Enzymology*, pp. 112-115. Dover Publications, New York.

Kemp, B.E., Graves, D.J., Benjamini, E., & Krebs, E.G. (1977). Role of multiple basic residues in determining the substrate specificity of cyclic AMP-dependent protein kinase. *J. Biol. Chem. 252*, 4888-4894.

Knighton, D.R., Zheng, J., Ten Eyck, L.F., Ashford, V.A., Xuong, N.-H., Taylor, S.S., & Sowadski, J.M. (1991a). Crystal structure of the catalytic subunit of cAMP-dependent protein kinase. *Science 253*, 407-413.

Knighton, D.R., Zheng, J., Ten Eyck, V.A., Xuong, N.-H., Taylor, S.S., & Sowadski, J.M. (1991b). Structure of a peptide inhibitor bound to the catalytic subunit of cyclic adenosine monophosphate-dependent protein kinase. *Science 253*, 414-420.

Kong, C.-T. & Cook, P.F. (1988). Isotope partitioning in the adenosine 3'-5'-monophosphate dependent protein kinase reaction indicates a steady-state random kinetic mechanism. *Biochemistry 27*, 4795-4799.

Koshland, D.E. (1958). Application of a theory of enzyme specificity to protein synthesis. *Proc. Natl. Acad. Sci. USA 44*, 98-104.

Krebs, E.G. & Beavo, J.A. (1979). Phosphorylation-dephosphorylation of enzymes. *Annu. Rev. Biochem. 48*, 923-959.

Olah, G.A., Mitchell, R.D., Sasnick, T.R., Walsh, D.A., & Trewhalla, J. (1993). Solution structure of the cAMP-dependent protein kinase catalytic subunit and its contraction upon binding the protein kinase inhibitor peptide. *Biochemistry 32*, 3649-3657.

Qamar, R., Yoon, M.-Y., & Cook, P.F. (1992). Kinetic mechanism of the adenosine 3'-5'-monophosphate dependent protein kinase catalytic subunit in the direction of magnesium adenosine 5'-diphosphate phosphorylation. *Biochemistry 31*, 9986-9992.

Reed, J., Kinzel, V., Kemp, B.E., Cheung, H.-C., & Walsh, D.A. (1985). Circular dichroic evidence for an ordered sequence of ligand/binding site interactions in the catalytic reaction of the cAMP-dependent protein kinase. *Biochemistry 24*, 2967-2973.

Salerno, A., Mendelow, M., Prorok, M., & Lawrence, D.S. (1990). Noncovalent active site interactions enhance the affinity and control the binding order of reversible inhibitors of the cAMP-dependent protein kinase. *J. Biol. Chem. 265*, 18079-18082.

Segel, I.H. (1975). *Enzyme Kinetics, Behavior and Analysis of Rapid Equilibrium and Steady-State Enzyme Systems*, p. 109. Wiley, New York.

Whitehouse, S., Feramisco, J.R., Casnellie, J.E., Krebs, E.G., & Walsh, D.A. (1983). Studies on the kinetic mechanism of the catalytic subunit of the cAMP-dependent protein kinase. *J. Biol. Chem. 258*, 3693-3701.

Yonemoto, W.M., McGlone, M.L., Slice, L.W., & Taylor, S.S. (1991). Prokaryotic expression of the catalytic subunit of cAMP-dependent protein kinase. *Methods Enzymol. 200*, 581-596.

Zetterqvist, O., Ragnarsson, U., & Engstrom, L. (1990). Substrate specificity of cyclic AMP-dependent protein kinase. In *Peptides and Protein Phosphorylation* (Kemp, B.E., Ed.), pp. 171-187. CRC Press, Inc., Boca Raton, Florida.

Zheng, J., Knighton, D.R., Ten Eyck, V.A., Karlsson, R., Xuong, N.-H., Taylor, S.S., & Sowadski, J.M. (1993a). Crystal structure of the catalytic subunit of cAMP-dependent protein kinase complexed with MgATP and peptide inhibitor. *Biochemistry 32*, 2154-2161.

Zheng, J., Trafny, E.A., Knighton, D.R., Ten Eyck, V.A., Xuong, N.-H., Taylor, S.S., & Sowadski, J.M. (1993b). 2.2 Å refined crystal structure of the catalytic subunit of cAMP-dependent protein kinase complexed with MnATP and a peptide inhibitor. *Acta Crystallogr. D49*, 362-365.